Complete set of types of phase transition in generalized heterogeneous k-core percolation

Huiseung Chae, Soon-Hyung Yook,* and Yup Kim†
Department of Physics and Research Institute for Basic Sciences, Kyung Hee University, Seoul 130-701, Korea
(Received 16 December 2013; published 22 May 2014)

We study heterogeneous k-core (HKC) percolation with a general mixture of the threshold k, with $k_{\min} = 2$ on random networks. Based on the local tree approximation, the scaling behaviors of the percolation order parameter $P_\infty(p)$ are analytically obtained for general distributions of the threshold k. The analytic calculations predict that the generalized HKC percolation is completely described by the series of continuous transitions with order parameter exponents $\beta_n = 2/n$, discontinuous hybrid transitions with $\beta_H = 1/2$ or $\beta_{A_4} = 1/4$, and three kinds of multiple transitions. Simulations of the generalized HKC percolations are carried out to confirm analytically predicted transition natures. Specifically, the exponents of the series of continuous transitions are shown to satisfy the hyperscaling relation $2\beta_n + \gamma_n = \bar{\nu}_n$.

DOI: 10.1103/PhysRevE.89.052134 PACS number(s): 64.60.ah, 64.60.aq, 05.70.Fh, 89.75.Da

I. INTRODUCTION

The structural transitions in complex networks have attracted many researchers in various scientific areas due to their profound physical implications and wide range of important applications [1–4]. Recently, k-core (KC) percolation [5–8] and heterogeneous k-core (HKC) percolation [9–13] have been intensively studied. As the generalized concept of the giant component, KC gives a deeper insight into the structure and organization of complex networks [10,11]. KC percolation is relevant to understanding the resilience of a network under random damage [12]. KC percolation was also found to be applied to important research fields, such as protein-interaction networks [14], jamming [15], and neural networks [16]. The KC on a network is defined as the maximal cluster or the giant component in which each node is directly linked to at least k nodes within the cluster itself [6–8]. Here k is often called the threshold k. In statistical physics, it is very important to find new universality classes of phase transition. In this sense KC percolation is also theoretically very important, because two novel transitions which cannot exist in ordinary percolation were found. One was the continuous transition in two-core percolation [5–8], whose critical phenomena belong to the same universality class as the biconnecting percolation [17]. The other was a special type of discontinuous transition, the so-called hybrid transition, which occurs in KC percolation with $k \geqslant 3$ [5–7].

In spite of wide applications and theoretical merits, KC percolation has intrinsic limitations. In real systems, some individuals are more resilient than others, and thus some nodes remain in the core structure with fewer neighbors than others. However, in KC percolation, the threshold k of any node is identical. As a natural extension, HKC percolation was introduced to overcome intrinsic limitation [10]. HKC on a network is also defined as the maximal cluster in which each node i has its own threshold k_i and has at least k_i directly linked neighbors within the cluster itself [10]. Moreover, HKC percolation with generalized thresholds was also found to have more wide applications to various fields, such as opinion formations [18], epidemic spreading [19], robustness of network [9–12].

Until now, HKC percolations were mainly studied by using binary mixtures of k on complex networks [10–12]. In these studies it was argued that there are two additional transitions which had not been found in KC percolation. One was the multiple transitions, first showing the continuous transition, and later the discontinuous hybrid transition. The other was the continuous transition with so-called tricritical phenomena [11]. HKC percolation with a trinary mixture of k with $k_i \geqslant 3$ on random networks was also investigated to show different types of hybrid transitions [13]. However, these studies on HKC percolation with the binary mixtures [10–12] and the trinary mixture [13] of k are far from the completion because of the following reasons. First of all, one should study HKC percolation with general mixtures of k_i in which there probably exists a much richer variety of transition natures. Furthermore, the previous studies [10–13] were based mainly on the analysis of order parameter. To decide the universality class of a continuous transition exactly and to confirm the analytically suggested transition natures numerically, one should need other physical properties such as the susceptibility in addition to the order parameter. The only research on the susceptibility of HKC percolation until now was a numerical study to understand the tricritical phenomena for the binary mixture of k [11]. They used the corona cluster to obtain the susceptibility exponent γ [8,10,11]. However, the corona cluster is a very special cluster in which each node i has exactly k_i directly linked neighbors, and thus the analysis based on the corona cluster might not be an effective method to obtain the susceptibility exponent γ in HKC percolation with general mixtures of k_i. So one needs another framework to calculate γ.

In this paper, HKC percolations with general mixtures of k_i on Erdös-Rényi networks are studied to find the complete set of phase transition natures at the mean-field level. Using the local tree approximation [10–13], the transition natures depending on probabilities assigned to the k_i values are analytically derived. The complete set of possible transition natures in generalized HKC percolations consists of a series of continuous transitions with the order parameter exponent $\beta_n = 2/n$ ($n = 1,2,3,\ldots$), discontinuous hybrid transitions, and multiple transitions.

*syook@khu.ac.kr
†Corresponding author: ykim@khu.ac.kr

The local tree approximation mainly calculates the order parameter exponent β [10–12]. To decide the universality class of a continuous transition precisely and to confirm the analytically suggested transition natures numerically, simulations on HKC percolation are performed. Since HKC percolation considers only the maximal (giant) cluster, we use the fluctuation of the order parameter as the susceptibility. The fluctuation of the order parameter has widely been used to calculate γ in studies on the various percolation problems [20–24] as well as the mean size of finite clusters [25].

Using the finite-size scaling ansatz of the order parameter and the susceptibility, the analytically predicted transition natures are confirmed by numerical simulations. Specifically, the nth universality class with the hyperscaling relation $2\beta_n + \gamma_n = \bar{\nu}_n$ is numerically confirmed at the theoretically predicted combination of assigned probabilities to k_i values.

II. ANALYTIC RESULTS

Let us consider a network with N nodes. Each node i on the network is assumed to have a quenched integer threshold k_i. Then the HKC on the network is defined as the maximal cluster in which each node i is directly linked to at least k_i nodes in the cluster itself. We here consider HKC percolation based on site (node) dilution. In HKC percolation, nodes of a given network are randomly removed with probability $1-p$ and one determines how the fraction of occupied nodes, $P_\infty(p)$, in HKC varies as p is decreased [10–12]. The HKC percolation transition thus means the transition from the state with $P_\infty(p) > 0$ (ordered state) to that with $P_\infty(p) = 0$ (disordered state). HKC percolation on random networks [26] with the degree distribution $P(q) = e^{-\langle q\rangle}\langle q\rangle^q/q!$ is now considered. The probability r_k for a node to have the threshold k must satisfy the normalization condition $\sum_{k=k_{\min}}^{k_{\max}} r_k = 1$, where $k_{\max}$ ($k_{\min}$) is the maximal (minimal) of k_i. The HKC percolation with $k_{\min} = 1$ has already been studied at a deeper level [10,12]. Thus in this paper we focus on the transition natures for the cases with $k_{\min} = 2$.

In the local tree approximation [10–12], a (k_i-1)-ary subtree rooted at i is the tree in which each occupied node j in the subtree has at least (k_j-1) occupied child nodes. Let $Z(p)$ be the probability that a randomly chosen node i is the root of a (k_i-1)-ary subtree for given p. Then, $P_\infty(p)$ has been shown to be written as [10–12]

$$P_\infty(p) = p\sum_{k=k_{\min}}^{k_{\max}} r_k \sum_{q=k}^{\infty} P(q) \sum_{l=k}^{q} \binom{q}{l} Z^l (1-Z)^l, \qquad (1)$$

and $Z(p)$ has been shown to satisfy the self-consistent equation [10–12]

$$Z = p\sum_{k=k_{\min}}^{k_{\max}} r_k \sum_{q=k}^{\infty} \frac{qP(q)}{\langle q\rangle} \sum_{l=k-1}^{q-1} \binom{q-1}{l} Z^l (1-Z)^{q-1-l}. \qquad (2)$$

Equation (2) has only the trivial solution $Z(p) = 0$ in the disordered state. In the ordered state, Eq. (2) should additionally have the nontrivial solution $Z(p) > 0$, which satisfies

$$p = 1/f(Z), \qquad (3)$$

where

$$f(Z) = \frac{1}{Z}\sum_{k=k_{\min}}^{k_{\max}} r_k \sum_{q=k}^{\infty} \frac{qP(q)}{\langle q\rangle} \sum_{l=k-1}^{q-1} \binom{q-1}{l} Z^l (1-Z)^{q-1-l}. \qquad (4)$$

Equation (3) should have a unique physical solution $Z(p)$ in the ordered state or $p > p^*$, whereas it does not have any solution $Z(p)$ in the disordered state. The HKC is defined as the maximal cluster under the given conditions. Therefore the physical solution $Z(p)$ in the ordered state should be the largest solution of Eq. (3) in the range $0 \leqslant Z \leqslant 1$. The HKC percolation threshold p^* thus satisfies $p^* = 1/f(Z^*)$, where $f(Z^*)$ is the global maximum of $f(Z)$. A continuous transition occurs when $Z^* = 0$. In contrast, a discontinuous transition occurs when $Z^* > 0$.

Let us first consider a trinary mixture of $k_i \in \{2,3,4\}$. From the condition $\sum_{k=2}^{4} r_k = 1$, r_k's are described by two parameters as $r_2 = r$, $r_3 = (1-r)s$, and $r_4 = (1-r)(1-s)$. Then $f(Z)$ for the trinary mixture can be written as the compact form

$$f(Z) = \frac{1-e^{-\langle q\rangle Z}}{Z} - \langle q\rangle(1-r)e^{-\langle q\rangle Z}\left[1 + \langle q\rangle\frac{1-s}{2}Z\right]. \qquad (5)$$

From Eq. (5), we find seven different typical functional forms of $f(Z)$ depending on r and s, as shown in Fig. 1(b). In the region D1, $f'(Z=0) > 0$ and $Z^* > 0$. On the curve d, $f'(Z=0) = 0$, $f''(Z=0) > 0$, and $Z^* > 0$. In the region D2, $f'(Z^*) = 0$, $f''(Z^*) < 0$, and $Z^* > 0$. Therefore, in the slashed region of Fig. 1(a), including D1 $[s > r/(1-r)]$, D2, and d $(s = r/(1-r) < 1/2)$, discontinuous transitions occur because $Z^* > 0$. It is confirmed that the discontinuous transitions are all the same type of a hybrid transition with $P_\infty(p) - P_\infty[p^*(r,s)] \propto (p-p^*)^{\beta_H}$ with $\beta_H = 1/2$, as already found on the lines $s = 1(r < 1/2)$ and $s = 0(r < 0.223\,996\ldots)$ [12].

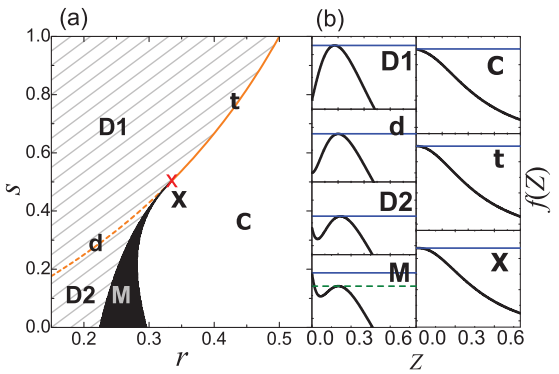

FIG. 1. (Color online) (a) Set of transition natures of HKC percolation with the trinary mixture of $k_i \in \{2,3,4\}$ on random networks with $\langle q\rangle = 10$, depending on r and s. In the slashed region of D1, D2, and d, discontinuous hybrid transitions with $\beta_H = 1/2$ occur. In C the transition is continuous with $\beta_1 = 2$. On curve t continuous transitions with $\beta_2 = 1$ occur. At point X continuous transition with $\beta_3 = 2/3$ occurs. In M, multiple transitions occur. (b) Typical forms of $f(Z)$ corresponding to the regions, curves, and the point of r and s. The horizontal solid line in each graph stands for $1/p^*$ and the dashed line denotes $1/p_\ell$.

In contrast, continuous transitions occur in the region C, satisfying two conditions, $s < r/(1-r)$ and $f'(Z) < 0$. To understand the transition nature of HKC percolation, a power series expansion of $f(Z)$ around $Z = 0$,

$$f(Z) = \langle q\rangle r - a_1 \frac{\langle q\rangle^2}{2!} Z + a_2 \frac{\langle q\rangle^3}{3!} Z^2 + \cdots, \tag{6}$$

is considered, where $a_1 = r - s + rs$, $a_2 = 1 - 3s + 4rs$, and so on. In the region C, $a_1 > 0$, $f'(0) < 0$, and $Z^* = 0$; thus $Z(p) \propto (p - p^*)$ with $p^* = 1/\langle q\rangle r$. Moreover, in the region C, $f(Z)$ is a monotonic decreasing function as shown in Fig. 1(b), and thus

$$P_\infty(p) \propto (p - p^*)^{\beta_1} \tag{7}$$

with $\beta_1 = 2$, because

$$P_\infty(p) = p \frac{\langle q\rangle^2 r}{2} [Z(p)]^2 + p \frac{\langle q\rangle^3 (s - r + rs)}{3!} [Z(p)]^3 + \cdots \tag{8}$$

in the limit $p \to p^{*+}$. The universality class with $\beta_1 = 2$ was first found in the biconnecting percolation [17] and later in the two-core percolation [5–8,12]. Let us call this universality class the *1st universality class* in HKC percolation.

On the curve t ($s = r/(1-r) > 1/2$), $f'(0) = 0$ and $f'(Z) < 0$ for $0 < Z \leqslant 1$. Thus on the curve t, $f(Z) = \langle q\rangle r + [a_2 \langle q\rangle^3 Z^2]/3! + \cdots$ and one can obtain $Z(p) \propto (p - p^*)^{1/2}$ with $p^* = 1/\langle q\rangle r$. Therefore

$$P_\infty(p) \propto (p - p^*)^{\beta_2} \tag{9}$$

with $\beta_2 = 1$, and this continuous transition was first found for $r = 1/2$ and $s = 1$ [11]. The universality class with $\beta_2 = 1$ should be called the *2nd universality class*.

In the remaining region M of Fig. 1(a) between C and D2, a local maximum $f[Z^*_\ell(p_\ell) > 0]$ with $f'(Z^*_\ell) = 0$ and $f''(Z^*_\ell) < 0$ exists, even though $f[Z^*(p^*) = 0]$ should be the global maximum [see $f(Z)$ of M in Fig. 1(b)]. Because $p^* < p_\ell$, the multiple transitions (i.e., the continuous transition with $\beta_1 = 2$ first occurs at $p = p^*$ and the discontinuous hybrid transition with $\beta_H = 1/2$ follows at $p = p_\ell$) occur in the region M, as shown on the line $s = 0$ and $0.223\,996\cdots < r < 0.296\,3$ [12]. We call these transitions *type-1 multiple transitions*.

Finally, an anomalous continuous transition occurs at the boundary point X ($r = 1/3$ and $s = 1/2$, or $r_2 = r_3 = r_4$), where the curve t and the region M cross. At X, $f'(0) = f''(0) = 0$ and $f'(Z) < 0$ for $0 < Z \leqslant 1$. Therefore $Z(p) \propto (p - p^*)^{1/3}$ with $p^* = 1/\langle q\rangle r$, and

$$P_\infty(p) \propto (p - p^*)^{\beta_3} \tag{10}$$

with $\beta_3 = 2/3$. This universality class with $\beta_3 = 2/3$ should be *the 3rd universality class*.

Other transition natures arise for the general mixture of k_i. Let us consider the mixture of $k_i \in \{2,3,4,5\}$. Similarly to the previous trinary mixture, r_k's are described by three parameters as $r_2 = r, r_3 = (1-r)s, r_4 = (1-r)(1-s)u$, and $r_5 = (1-r)(1-s)(1-u)$. Depending on the parameter u, two sets of transition natures are found. For $u \geqslant 1/2$, the set of transition natures is the same as that in Fig. 1, but the boundaries are shifted depending on r, s, and u. We call this set *the first set* of transition natures. In this set the curve t and the region M cross at the point X [$r = u/(1+2u)$ and $s = u/(1+u)$, or $r_2 = r_3 = r_4$]. At the point X [$r = u/(1+2u)$ and $s = r/(1-r) = u/(1+u)$, or $r_2 = r_3 = r_4$], $f(Z)$ can be written as

$$f(Z) = \langle q\rangle r - \frac{\langle q\rangle^4}{4!} \frac{2u-1}{1+2u} Z^3 + \cdots. \tag{11}$$

For $u > 1/2$ the critical phenomena at point X in the first set belong to the third universality class with $\beta_3 = 2/3$ as in Fig. 1. In contrast, if $u = 1/2$, $f'(0) = f''(0) = f'''(0) = 0$ and

$$P_\infty(p) \propto (p - p^*)^{\beta_4} (\beta_4 = 1/2) \tag{12}$$

at point X. Thus the continuous transition at point X for $u = 1/2$ belongs to another universality class, or the *4th universality class*.

On the other hand, for $u < 1/2$, the special point X does not appear, but the region M crosses the part of the curve t between two points t_L and t_R, as shown in Fig. 2(a). At the point t_R, the inflection point of $f(Z)$ exists at $Z = Z_I (> 0)$ or $f'(Z_I) = f''(Z_I) = 0$, as shown in Fig. 2(b). At the point t_L, $f(0) = f(Z^* > 0)$ and $f'(0) = 0$. On the part of curve t between t_L and t_R, a local maximum $f[Z^*_\ell(p_\ell) > 0]$ exists, even though $f[Z^*(p^*) = 0]$ should be the global maximum. Since $p^* < p_\ell$ and $f'(0) = 0$, the continuous transition with $\beta_2 = 1$ first occurs at $p = p^*$. Then a discontinuous hybrid transition with $\beta_H = 1/2$ also occurs at $p = p_\ell$. Thus, on that part of the curve new multiple transitions, which are distinct from the multiple transitions in the region M with $\beta_1 = 2$, occur. We call these new transitions *type-2 multiple transitions*. In addition, *multiple discontinuous transitions* occur in the region M_D. As shown in Fig. 2(b), $f(Z)$ in the region M_D has two maxima, $f(Z^*_1)$ and $f(Z^*_2)$, with the condition $f(Z^*_1) > f(Z^*_2)$ for $Z^*_1 < Z^*_2$. Therefore the first in M_D is a hybrid transition with $\beta_H = 1/2$ from nonpercolating phase to HKC percolating phase. The second is also a transition with $\beta_H = 1/2$ between low-k phase and a high-k phase [13]. At a special point A_4 on the boundary between D1 and M_D, another transition nature called the A_4 singularity [13] occurs.

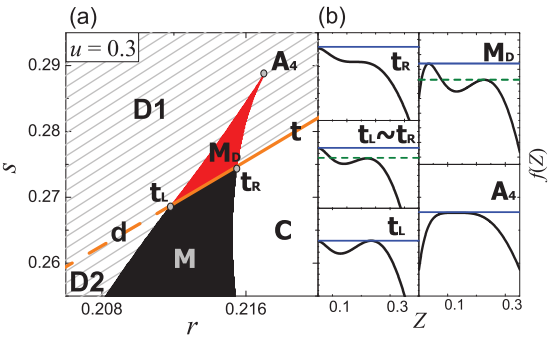

FIG. 2. (Color online) (a) Set of transition natures of HKC percolation with the mixture of $k_i \in \{2,3,4,5\}$ for $u = 0.3 (< 1/2)$. The region M meets the part of curve t between t_L and t_R. On part of the curve, multiple transitions occur as in the region M, but the continuous transition of multiple transitions has $\beta_2 = 1$. In the region M_D, multiple discontinuous transitions occur. (b) $f(Z)$'s at points t_R, t_L, and A_4. The typical forms of $f(Z)$ on the part of the curve between t_L and t_R and in M_D.

At A_4, $f'(Z^*) = f''(Z^*) = f'''(Z^*) = 0$ holds. The A_4 singularity indicates the hybrid transition as $P_\infty(p^*) \propto (p - p^*)^{\beta_{A_4}}$ with $\beta_{A_4} = 1/4$. For a given $u(< 1/2)$, the A_4 singularity appears at a unique point on a two-parameter rs plane. For example, the A_4 singularity occurs at the combination $\{r = 0.217\,06\ldots, s = 0.288\,78\ldots, u = 0.3\}$, as shown in Fig. 2(a). In the limit $u \to 1/2^-$, the point A_4 approaches the point $(r = 1/4, s = 1/3)$. The boundary of M_D between t_R and A_4 can be determined by the condition that $f(Z)$ has one inflection point at $Z = Z_I(> Z^*)$, or $f'(Z_I) = f''(Z_I) = 0$. On the boundary of M_D between A_4 and t_L, $f(Z_1^*) = f(Z_2^*)$ with $Z_2^* > Z_1^* > 0$ holds. Therefore, for $u < 1/2$, the second set of transition natures is composed of continuous transitions with $\beta_1 = 2$ or $\beta_2 = 1$, the hybrid transitions with $\beta_H = 1/2$ or $\beta_{A_4} = 1/4$, and three types of multiple transitions.

For the general mixture of $k_i \in \{2,3,4,\ldots,k_{\max}\}$, the first set of transition natures as Fig. 1(a) appears if the special point X exists. Otherwise, the second set as Fig. 2(a) appears. The conditions of the existence of the point X are $r_2 = r_3 = r_4$ and $Z^* = 0$. r_k's for the general mixture can also be parameterized as $r_2 = r$, $r_3 = (1-r)s$, $r_4 = (1-r)(1-s)u$, $r_5 = (1-r)(1-s)(1-u)t$, and $\sum_{k=6}^{k_{\max}} r_k = (1-r)(1-s)(1-u)(1-t)$. If $r_2 = r_3 = r_4$, or $r = u/(1+2u)$ and $s = r/(1-r) = u/(1+u)$, $f(Z)$ in Eq. (4) for the general mixture is expanded as

$$f(Z) \simeq \langle q\rangle r + \frac{\langle q\rangle^4}{4!}\frac{t - tu - u}{1+2u}Z^3 + \cdots \tag{13}$$

when $Z \to 0^+$. Therefore, if $u < t/(t+1)$, $f'(0) = f''(0) = 0, f'''(0) > 0$, and $Z^* > 0$. Thus when $u \geqslant t/(t+1)$, the point X exists and the first set of transition natures appears. When $u < t/(t+1)$, the point X does not exist and the second set of transition natures appears. As for the mixture $k_i \in \{2,3,4,5\}$, only two sets of transition natures as Figs. 1(a) and 2(a) appear for the general mixture and no further different set appears.

For the general mixture of $k_i \in \{2,3,4,\ldots,k_{\max}\}$, there exists an essential difference compared to the transition natures for the mixture of $k_i \in \{2,3,4,5\}$. The essential difference is the transition nature at the special point X when $u = t/(1+t)$, and the nature depends on $r_6, r_7, \ldots, r_{k_{\max}}$. Equation (4) can be written as

$$f(Z) = \sum_{l=0}^{\infty} b_l Z^l, \tag{14}$$

where $b_l = \frac{l+2}{\langle q\rangle}\sum_{q=l}^{\infty}\binom{q}{l+2}P(q)\sum_{k=0}^{l}\binom{l}{k}r_{k+2}(-1)^{l+k}$. From Eq. (14), $f(0) - f(Z) \propto Z^n$ when $r_2 = r_3 = \cdots = r_{n+1}$. Furthermore,

$$f'(Z) = -\frac{e^{-\langle q\rangle Z}}{Z^2}\sum_{k=2}^{\infty}\frac{\langle q\rangle^k Z^k}{k!}\left[\sum_{l=2}^{k}(r_l - r_{k+1})\right], \tag{15}$$

and thus $f'(Z) < 0$ when $r_2 = r_3 = \cdots = r_{n+1}$ and $r_2 > r_k$ for $k > n+1$. Therefore, *the nth universality class* with

$$P_\infty \propto (p - p^*)^{\beta_n}(\beta_n = 2/n) \tag{16}$$

appears at the point X when $r_2 = r_3 = \cdots = r_{n+1}$ and $r_2 > r_k$ for $k > n+1$, because $f(Z)$ is a monotonic decreasing function and $Z \propto (p - p^*)^{1/n}$ with $p^* = 1/\langle q\rangle r$.

Except the transition nature at the point X, the transition natures are mainly dependent upon r, s, u, and t [or $r_k(k \leqslant 5)$], even though the boundaries in Figs. 1(a) and 2(a) slightly move as r_k values for $k > 5$ vary. This result physically means that r_k's with relatively smaller k affect the transition nature more strongly than r_k's with relatively larger k. When $r > 0.5$, for instance, only the 1st universality class appears, regardless of the values of s, u, t, etc.

III. NUMERICAL SIMULATIONS

To confirm the analytically derived transition natures in HKC percolation, the numerical simulations on random networks are performed. First, random networks with N nodes and $\langle q\rangle = 10$ are constructed by the Erdös-Rényi model [26]. Then a threshold k_i is assigned to each node i in accordance with the probability r_{k_i}. Each node is removed with probability $1 - p$, and the HKC is extracted by the following algorithm: (i) Remove every node i that has fewer occupied neighbors than k_i. (ii) Some of survived nodes may remain with fewer survived neighbors than their thresholds. Then remove these nodes. Repeat this process until no further removal is possible. (iii) The largest remaining cluster is the HKC for the given p.

Then $P_{\max}(p,N) \equiv \langle s_{\max}(p,N)\rangle / N$ and $P_\infty(p) = \lim_{N\to\infty} P_{\max}(p,N)$, where $s_{\max}(p,N)$ is the number of nodes in the HKC. To decide a universality class precisely, we consider the fluctuation of the order parameter

$$\chi(p,N) = \frac{\langle s_{\max}^2\rangle - \langle s_{\max}\rangle^2}{N} \tag{17}$$

as the susceptibility [20,22–24], which scales as $\chi(p) = \lim_{N\to\infty}\chi(p,N) \sim (p - p^*)^{-\gamma}$ in a continuous transition. Since the dimension of random networks is infinite [26], $\chi(p,N)$ and $P_{\max}(p,N)$ in a continuous transition should satisfy finite-size scaling ansatz

$$\chi(p,N) = N^{\gamma/\bar\nu}G[(p - p^*)N^{1/\bar\nu}] \tag{18}$$

and

$$P_{\max}(p,N) = N^{-\beta/\bar\nu}F[(p - p^*)N^{1/\bar\nu}], \tag{19}$$

where $\bar\nu = d_c\nu$ [25]. Therefore, from the simulation data of $\langle s_{\max}(p,N)\rangle$ and $\langle s_{\max}^2(p,N)\rangle$ and the finite-size scaling ansatz, one can obtain β, γ, and $\bar\nu$ of a continuous transition, which must satisfy the hyperscaling relation $2\beta + \gamma = \bar\nu$.

For the mixture of $k_i \in \{2,3,4,5\}$ with $r_2 = r$, $r_3 = (1-r)s$, $r_4 = (1-r)(1-s)u$, and $r_5 = (1-r)(1-s)(1-u)$, the numerical simulations are carried out. $\chi(p,N)$ and $P_{\max}(p,N)$ are obtained for various combinations of $\{r,s,u\}$. Typical results are shown in insets of Figs. 3(a) and 3(b).

From the simulation data and the scaling ansatz, critical exponents are estimated to compare with the analytic results. For example, we estimate the critical exponents β_4, γ_4, and $\bar\nu_4$ at the point X $(r = 1/4, s = 1/3, u = 1/2)$ in the following way. The scaling ansatz (18) makes the maximal of $\chi(p,N)$ for the given N, $\chi_{\max}[p_{\max}(N),N]$, and $p_{\max}(N)$ at which $\chi(p,N)$ is maximal satisfy the relations

$$p_{\max}(N) - p^* \propto N^{-1/\bar\nu} \tag{20}$$

and

$$\chi_{\max}[p_{\max}(N),N] \propto N^{\gamma/\bar\nu}. \tag{21}$$

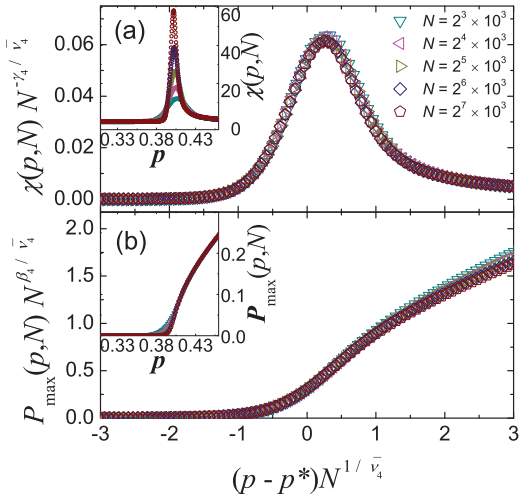

FIG. 3. (Color online) The numerical data confirming the 4th universality class for the mixture $k_i \in \{2,3,4,5\}$ when $r = 1/4$, $s = 1/3$, and $u = 1/2$. (a) Scaling collapse of $\chi(p,N)$ with $\bar{\nu}_4$ and γ_4 obtained from the fits in Figs. 4(a) and 4(b). Inset: Plot of $\chi(p,N)$ against p. (b) Scaling collapse of $P_{max}(p,N)$, with $\bar{\nu}_4$ and β_4 obtained from the fits in Figs. 4(a) and 4(c). Inset: Plot of $P_{max}(p,N)$ against p.

By fitting Eq. (20) to the simulation data of $p_{max}(N)$ as shown in Fig. 4(a), p^* and $\bar{\nu}_4$ are estimated as $p^* \simeq 0.400(2)$ and $\bar{\nu} \simeq 2.4(1)$. Similarly, $\gamma_4/\bar{\nu}_4 \simeq 0.57(2)$ is obtained using Eq. (21), as shown in Fig. 4(b). Finally, $\beta_4/\bar{\nu}_4 \simeq 0.21(1)$ is also obtained using Eq. (19) or

$$P_{max}(p^*) \propto N^{-\beta/\bar{\nu}}, \tag{22}$$

with $p^* = 0.400$ as in Fig. 4(c). Numerically obtained results, $\beta_4 \simeq 0.50(5)$ and $p^* \simeq 0.400(2)$, are very close to the analytically obtained results $\beta_4 = 1/2$ and $p^* = 1/\langle q\rangle r = 2/5$ at the point X ($r = 1/4, s = 1/3, u = 1/2$). Furthermore, the

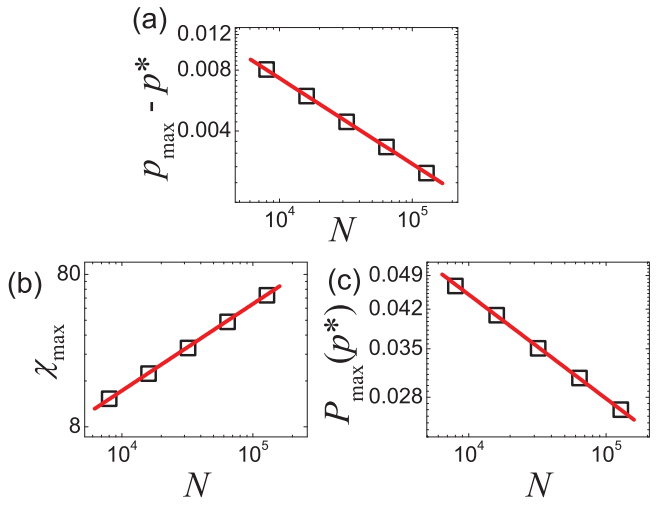

FIG. 4. (Color online) (a) Plot of $p_{max}(N) - p^*$ against N. $p^* \simeq 0.400(2)$ and $\bar{\nu}_4 \simeq 2.4(1)$ are estimated from $p_{max}(N) - p^*(\infty) \propto N^{-1/\bar{\nu}}$. (b) Plot of $\chi_{max}[p_{max}(N),N]$ against N. $\gamma_4/\bar{\nu}_4 \simeq 0.57(2)$ is estimated from $\chi_{max} \propto N^{\gamma/\bar{\nu}}$. (c) Plot of $P_{max}(p^*,N)$ against N. $\beta_4/\bar{\nu}_4 \simeq 0.21(1)$ is estimated from $P_{max}(p^*) \propto N^{-\beta/\bar{\nu}}$ with $p^* = 0.400$.

obtained exponents $\beta_4 \simeq 0.50(5)$, $\gamma_4 \simeq 1.37(9)$, and $\bar{\nu}_4 \simeq 2.4(1)$ will satisfy the hyperscaling relation $2\beta_4 + \gamma_4 = \bar{\nu}_4$. Because β's from analytical results are fractional numbers and the exponents should be mean-field exponents, other critical exponents should physically be fractional numbers. The numerically obtained critical exponents are close to $\beta_4 = 1/2, \gamma_4 = 7/5$, and $\bar{\nu}_4 = 12/5$. As shown in Figs. 3(a) and 3(b), $P_{max}(p,N)$ and $\chi(p,N)$ satisfy the scaling relations Eqs. (18) and (19) with the exponents obtained in Fig. 4 very well.

The critical exponents of other universality classes are confirmed through the same numerical method. Exponents very close to $\beta_1 = 2, \gamma_1 = -1$, and $\bar{\nu}_1 = 3$ are obtained at two combinations, $\{r = 1/2, s = 1/2, u = 1\}$ and $\{r = 2/5, s = 1/5, u = 1\}$ in region **C**. This set of exponents confirms the 1st universality class and is the same set as that obtained from the mean-field theory of biconnecting percolation [17]. The set of exponents close to $\beta_2 = 1, \gamma_2 = 1$, and $\bar{\nu}_2 = 3$, which confirm the 2nd universality class, is obtained at two combinations $\{r = 2/5, s = 2/3, u = 1\}$ and $\{r = 3/8, s = 3/5, u = 1\}$ on curve t. The set of exponents close to $\beta_3 = 2/3, \gamma_3 = 4/3$, and $\bar{\nu}_3 = 8/3$ is obtained exactly at the point X ($r = 1/3, s = 1/2, u = 1$) and confirms the 3rd universality class. Finally, the set of exponents close to $\beta_4 = 1/2, \gamma_4 = 7/5$, and $\bar{\nu}_4 = 12/5$ is obtained exactly at the point X ($r = 1/4, s = 1/3, u = 1/2$) from the simulation data, as shown in Fig. 3. This set of exponents confirms the 4th universality class. All the sets of critical exponents obtained from simulations satisfy the hyperscaling relation $2\beta_n + \gamma_n = \bar{\nu}_n$ very well. In this way, one can confirm the analytically predicted series of universality classes with $\beta_n = 2/n$ as well as the multiple transitions and discontinuous hybrid transitions at the analytically predicted combinations $\{r_k\}$ by the simulation.

IV. SUMMARY AND CONCLUSION

In summary, the analytic calculations and numerical simulations of generalized HKC percolation are performed. In the analytic calculations, the exact conditions for each transition nature are obtained. Furthermore, we show that the critical phenomena of continuous transitions in HKC percolation belong to one of the series of the universality classes with

TABLE I. Complete set of transition natures in HKC percolation. Exponents in each universality class satisfy the hyperscaling relation $2\beta + \gamma = \bar{\nu}$.

Continuous transition	β	γ	$\bar{\nu}$
1st universality class	$\beta_1 = 2$	$\gamma_1 = -1$	$\bar{\nu}_1 = 3$
2nd universality class	$\beta_2 = 1$	$\gamma_2 = 1$	$\bar{\nu}_2 = 3$
3rd universality class	$\beta_3 = 2/3$	$\gamma_3 = 4/3$	$\bar{\nu}_3 = 8/3$
4th universality class	$\beta_4 = 1/2$	$\gamma_4 = 7/5$	$\bar{\nu}_4 = 12/5$
⋮	⋮	⋮	⋮
nth universality class	$\beta_n = 2/n$	⋮	⋮
Dis. hybrid transition	$\beta_H = 1/2$ or $\beta_{A_4} = 1/4$		
Multiple transitions	$(\beta_1 = 2$ or $\beta_2 = 1) \to (\beta_H = 1/2)$ $(\beta_H = 1/2) \to (\beta_H = 1/2)$		

$\beta_n = 2/n$. The discontinuous hybrid transitions with $\beta_H = 1/2$ and $\beta_{A_4} = 1/4$ also occur. Multiple transitions which first show the continuous transition with $\beta_1 = 2$ (type-1) or $\beta_2 = 1$ (type-2) also occur, and later the hybrid transition. There are multiple discontinuous transitions with which first a hybrid transition with $\beta_H = 1/2$ occurs and later another hybrid with $\beta_H = 1/2$ transition also occurs. The numerical simulations of HKC percolation are also performed to confirm the series of universality classes and to find the other exponents, γ and $\bar{\nu}$. We also confirm that β, γ, and $\bar{\nu}$ for each universality class satisfy the hyperscaling relation $2\beta + \gamma = \bar{\nu}$. The complete set of transition natures in HKC percolation is displayed in Table I.

ACKNOWLEDGMENTS

This work was supported by a National Research Foundation of Korea (NRF) grant, funded by the Korean Government (MEST) (Grant No. 2011-0015257), and by the Basic Science Research Program through the National Research Foundation of Korea (NRF), funded by the Ministry of Education, Science and Technology (Grant No. 2012R1A1A2007430).

[1] Y.-Y. Liu, J.-J. Slotine, and A.-L. Barabási, Nature (London) **473**, 167 (2011).
[2] M. Weigt and A. K. Hartmann, Phys. Rev. Lett. **84**, 6118 (2000).
[3] M. Bauer and O. Golinelli, Phys. Rev. Lett. **86**, 2621 (2001).
[4] L. Zdeborová and M. Mézard, J. Stat. Mech. (2006) P05003.
[5] J. Chalupa, P. L. Leath, and G. R. Reich, J. Phys. C **12**, L31 (1979).
[6] S. N. Dorogovtsev, A. V. Goltsev, and J. F. F. Mendes, Phys. Rev. Lett. **96**, 040601 (2006).
[7] A. V. Goltsev, S. N. Dorogovtsev, and J. F. F. Mendes, Phys. Rev. E **73**, 056101 (2006).
[8] B. Corominas-Murtra, J. F. F. Mendes, and R. V. Solé, J. Phys. A **41**, 385003 (2008).
[9] G. J. Baxter, S. N. Dorogovtsev, A. V. Goltsev, and J. F. F. Mendes, Phys. Rev. E **82**, 011103 (2010).
[10] G. J. Baxter, S. N. Dorogovtsev, A. V. Goltsev, and J. F. F. Mendes, Phys. Rev. E **83**, 051134 (2011).
[11] D. Cellai, A. Lawlor, K. A. Dawson, and J. P. Gleeson, Phys. Rev. Lett. **107**, 175703 (2011).
[12] D. Cellai, A. Lawlor, K. A. Dawson, and J. P. Gleeson, Phys. Rev. E **87**, 022134 (2013).
[13] D. Cellai and J. P. Gleeson, Studies in Computational Intelligence **476**, 165 (2013).
[14] S. Wuchty and E. Almaas, Proteomics **5**, 444 (2005).
[15] J. M. Schwarz, A. J. Liu, and L. Q. Chayes, Europhys. Lett. **73**, 560 (2006).
[16] N. Chatterjee and S. Sinha, Prog. Brain Res. **168**, 145 (2007).
[17] A. B. Harris and T. C. Lubensky, J. Phys. A **16**, L365 (1983).
[18] D. J. Watts, Proc. Natl. Acad. Sci. USA **99**, 5766 (2002).
[19] J. P. Gleeson, Phys. Rev. E **77**, 046117 (2008).
[20] A. B. Harris and J. M. Schwarz, Phys. Rev. E **72**, 046123 (2005).
[21] T. Abete, A. de Candia, E. Del Gado, A. Fierro, and A. Coniglio, Phys. Rev. Lett. **98**, 088301 (2007).
[22] F. Radicchi and S. Fortunato, Phys. Rev. Lett. **103**, 168701 (2009).
[23] N. A. M. Araújo and H. J. Herrmann, Phys. Rev. Lett. **105**, 035701 (2010).
[24] N. Bastas, K. Kosmidis, and P. Argyrakis, Phys. Rev. E **84**, 066112 (2011).
[25] D. Stauffer and A. Aharony, *Introduction to Percolation Theory* (Taylor and Francis, London, 1991).
[26] R. Albert and A.-L. Barabási, Rev. Mod. Phys. **74**, 47 (2002).